Supporting Information

Stable and efficient planar Cu/Cu_2O film catalysts

Junfeng Yan*, Xu Meng

College of Textile and Garment, Key Laboratory of Clean Dyeing and Finishing Technology of Zhejiang Province, Shaoxing University, Shaoxing, 312000, Zhejiang, China

Experiment section

Chemicals and materials

These reagents used as received: Cupric Acetate Monohydrate($Cu(CH_3COO)_2$), Dodecyl sodium sulfonate($C_{12}H_{25}SO_4Na$), Cupric sulfate pentahydrate($CuSO_4\cdot5H_2O$), Sodium Hydroxide(NaOH), Sodium chloride(NaCl), potassium chloride(KCl), acetone(C_3H_6O), Acetic acid(CH_3COOH), Nickel(II) sulfate($NiSO_4\cdot6H_2O$), Boracic acid (H_3BO_4), p-Nitrophenol($C_6H_5NO_3$), $NH_3\cdot H_2O$ (2%). Indium tin oxide (ITO) glass (1 mm thickness, resistance valueless than 100 Ω) was obtained from Luoyang Guluo Glass Co. LTD. Deionized water was used for all aqueous solutions and washing. Other chemicals used were of analytical grade and were purchased from sigma Adrich.

Preparation of ITO substrate

ITO substrate was cleaned 10 minutes using a (KQ-100E) type ultrasonic cleaner from Kunshan Ultrasonic Instrument Company, using diluted ammonia, deionized water, ethanol and deionized water, respectively. The cleaned conductive glass was naturally dried in the air.

Characterization of Materials

X-ray diffraction(XRD). X-ray diffraction (XRD, Bruker D8 advance with Cu K〈 radiation) was used to characterize the phase composition.

Scanning electron microscope(SEM). Morphologies and structures of samples were researched by scanning electron microscope (Hitachi S-4800). SEM emits electrons through a field emission or thermal emission electron gun, focuses the electron beam with an electromagnetic lens, excites various signals from the sample, such as secondary electrons, absorbs electrons, etc, and then receives and magnifies them to form a scanned image that reflects the surface morphology.

X-ray photoelectron spectroscopy (XPS). The chemical composition and elemental state were obtained via XPS, which was collected by using a Thermo ESCALAB 250 instrument with a monochromated Al X-ray resource at 1486.6 eV.

UV-visible spectrophotometer(UV). UV-Vis spectra were deter mined on a UV-2550 spectrophotometer (Shimadzu, Japan).

BET surface area measurement. The surface area measurement was conducted on Autosorb-iQ (Quantachrome, USA).

Preparation of Cu/Cu_2O/ITO and Cu_2O/ITO Films

Initially, fixed the conductive glass on the electrode holder and immersed in the electrolyte, as the same time, adjust the distance between the auxiliary electrode and the working electrode is 2 cm, the substrate is immersed into 2 cm from top surface of the solution. This keeps the same conditions for all metal film preparation by electrodeposition. In this experiment, the electrochemical experiments were performed in a glass cell with a three-electrode configuration system consisting of an ITO substrate (1.0 cm*3.0 cm) as working electrode, a platinum wire as the counter electrode (CE) and a commercial reference electrode, saturated calomel electrode (SCE), all potentials given are *vs* $Hg/Hg_2Cl_2(s)/KCl$.

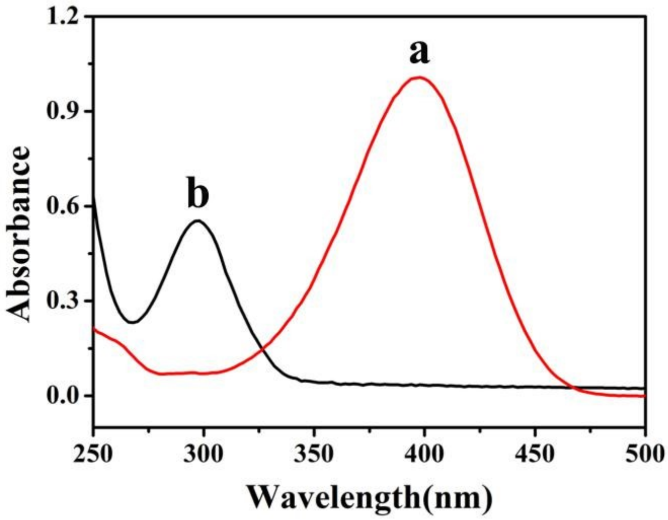

Fig. S1 UV-vis spectroscopy of 4-NP solution before (a) and after adding Cu_2O/Cu film catalysts (b).

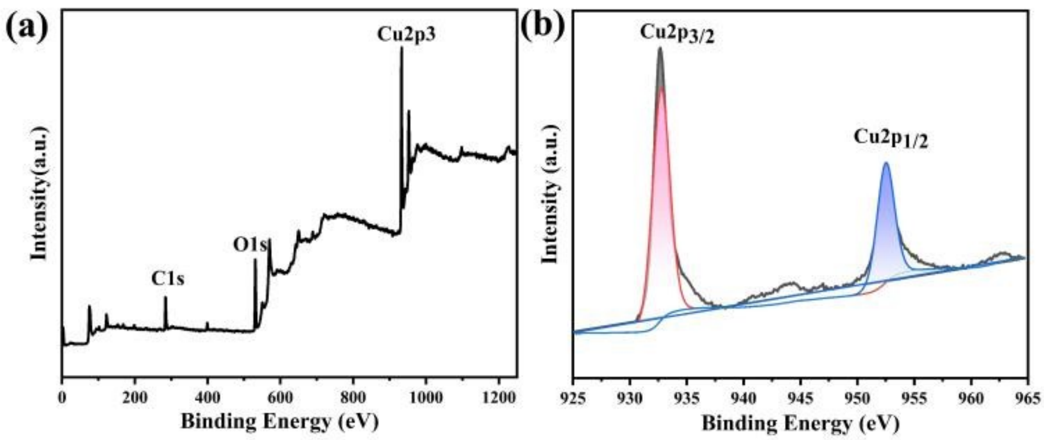

Fig. S2 (a)XPS spectra of the $Cu/Cu_2O/ITO$; (b) detailed spectrum of Cu_{2p}.

In order to investigate the elemental composition and valence states of the prepared $Cu/Cu_2O/ITO$ thin films, X-ray photoelectron spectroscopy was used. Fig. S2 (a) is full XPS spectrum of Cu/Cu_2O thin film that the signals of Cu, C and O elements are obviously. Fig. S2(b) is a fine spectrum of Cu_{2p} which corresponds to Cu^0 and Cu^{+1} at binding energy of 932.4 eV and 952.3 eV, respectively.

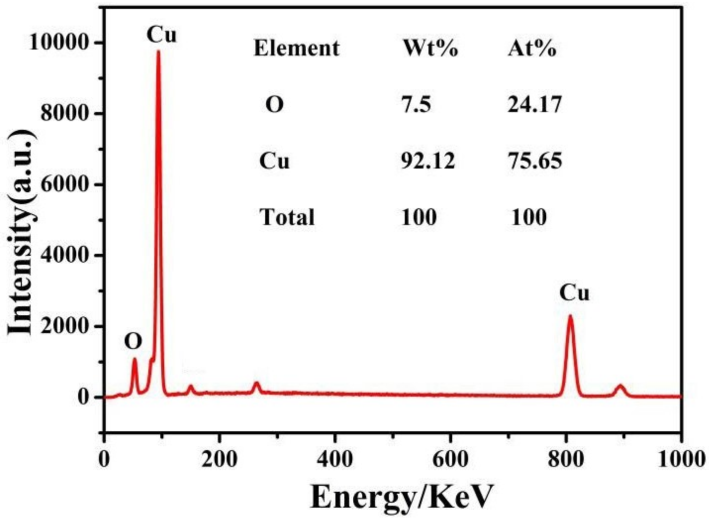

Fig. S3 EDS spectra of $Cu/Cu_2O/ITO$.

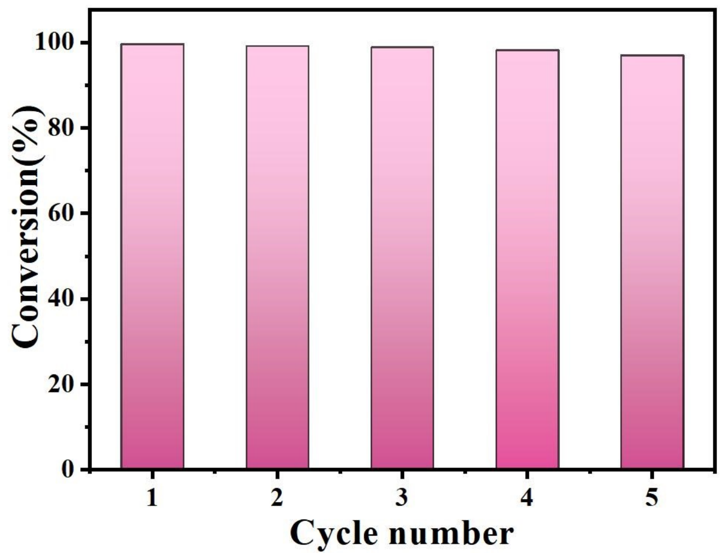

Fig. S4 Diagram of re-usability of $Cu/Cu_2O/ITO$ for catalytic degradation of 4-nitrophenol.

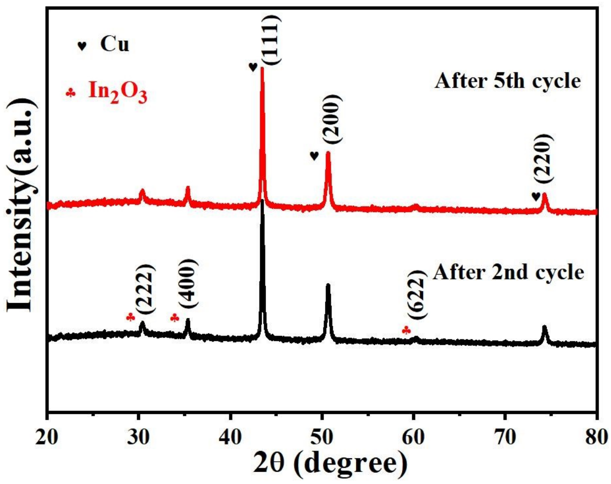

Fig. S5 XRD pattern of $Cu/Cu_2O/ITO$ films catalyzed reduction of 4-NP cycle reaction for repeating 5 times.

In order to evaluate the stability of the catalyst, we conducted XRD measurements after the catalyst was used for 5 times. As shown in Fig. S5, all diffraction peaks are consistent with the standard card of Cu, Cu_2O and In_2O_3, and the position and intensity of the diffraction peaks of the sample after two cycles and five cycles are consistent, indicating that the phase of the catalyst after two cycles and five cycles is basically unchanged, and no other impurities are formed on its surface.

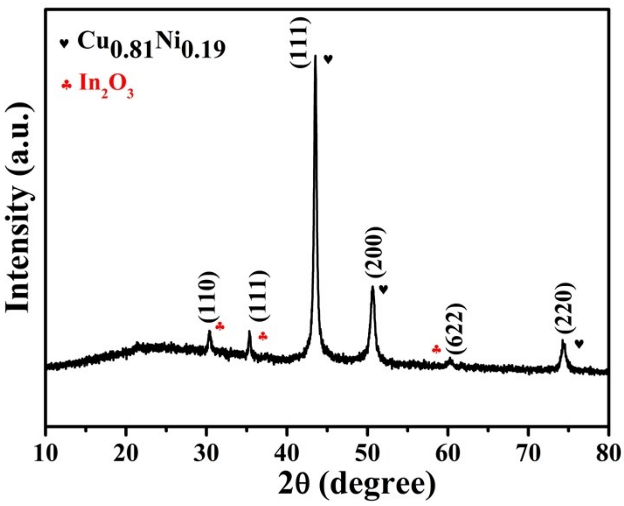

Fig. S6 XRD patterns of CuNi/ITO alloy film.

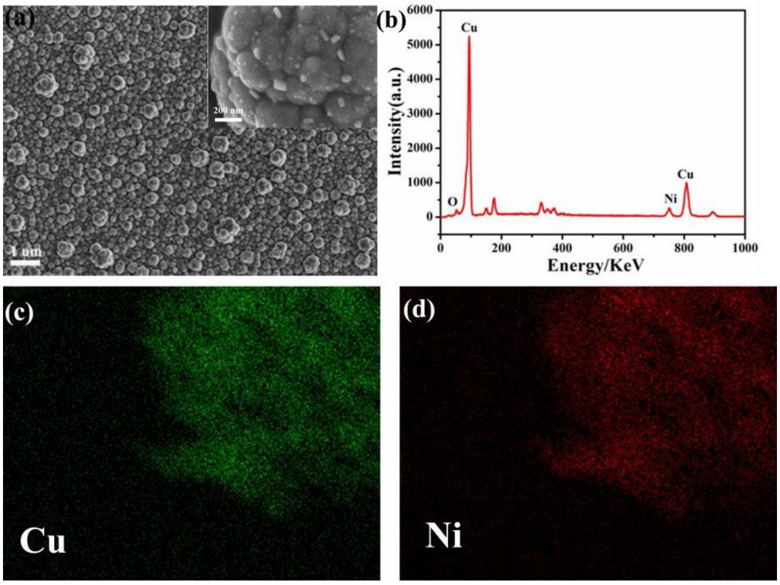

Fig. S7 (a) SEM images of the CuNi/ITO alloy film;(b) EDS of CuNi/ITO alloy;(c,d)EDS-mappings of CuNi/ITO alloy film.

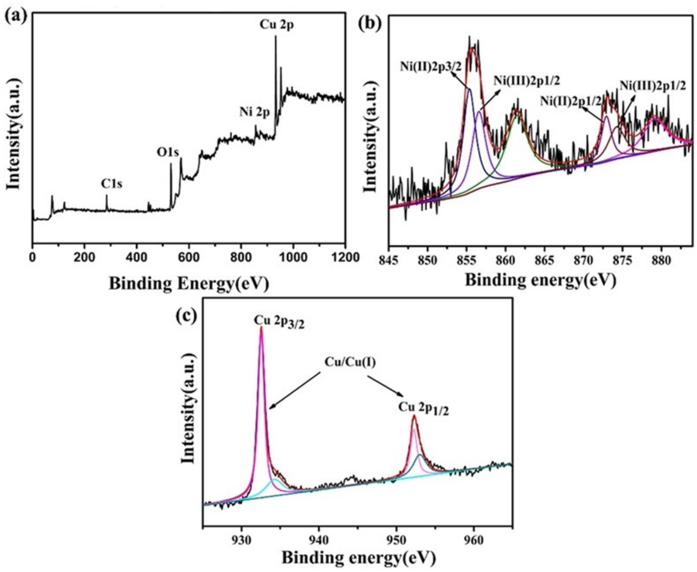

Fig. S8 (a) XPS analysis of the CuNi/ITO alloy materials; (b) High resolution XPS spectra of Ni(2p), Cu(2p).

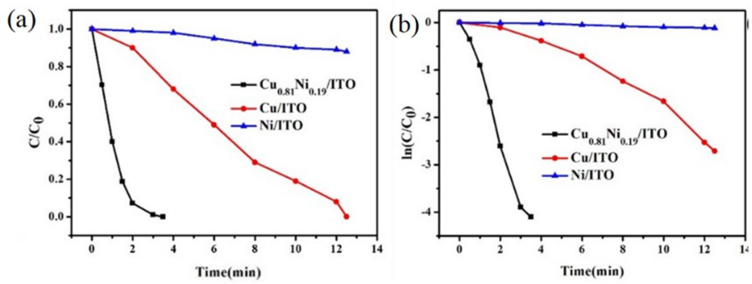

Fig. S9 (a) Plots of C/C_0 of 4-NP against time adding $Cu_{0.81}Ni_{0.19}$ and Cu catalysts; (b) Plots of $\ln(C/C_0)$ of 4-NP against time adding $Cu_{0.81}Ni_{0.19}$/ITO and Cu catalysts.

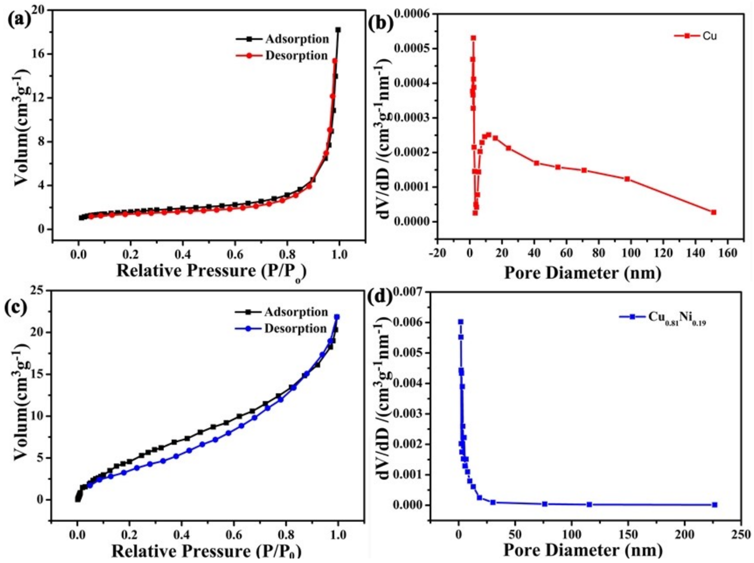

Fig. S10 Nitrogen Adsorption and Desorption curve (a); Pore size distribution curve of Cu (b) ; Nitrogen Adsorption and Desorption curve (c); Pore size distribution curve of $Cu_{0.81}Ni_{0.19}$ (d).

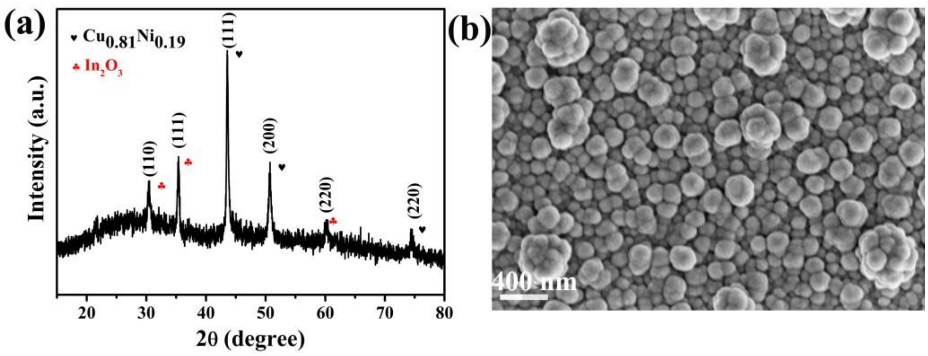

Fig. S11 $Cu_{0.81}Ni_{0.19}$/ITO alloy thin film material 4-NP cyclecatalyzed reduction after 5 times;(a) XRD; (b) SEM.

Catalysts	Concentration of 4-NP (mM)	Time (min)	K_{app} (min^{-1})	Ref.
Co_3O_4/HNTs	0.12	11	0.265	[1]
CuO-Ag	0.72	7	0.176	[2]
MnO_2	0.18	45	-----	[3]
Fe_2O_3/PS	0.072	90	-----	[4]
$FeVO_4$@CeO_2	0.14	30	0.163	[5]
NRGO-$CoWO_4$-Fe_2O_3	0.1	0.5	0.085	[6]
Ag_2S/TiO_2	0.12	50	0.080	[7]
CA-Ce/Zr@Cu	0.01	6	0.096	[8]

Au-Ag-G Hybrids	0.1	3.5	0.534	[9]
$Au_{1.0}Pd_{1.0}$ nanoalloy	0.2	16	0.239	[10]
Pal-NH_2@$Au_{48}Pd_{52}$	0.1	21	0.194	[11]
$InVO_4$/N-TiO_2	0.1	90	0.02	[12]
Cu_2O/ITO	**1**	**12**	**0.152**	**This work**
Cu/Cu_2O/ITO	**1**	**6**	**0.299**	**This work**
CuNi/ITO	**2**	**4.5**	**1.23**	**This work**

Table. S1 Comparison of the catalytic performance that of previously reported materials for the degredation of 4-nitrophenol (4-NP).

References

[1] Min Zhang, Xintai Su, Lida Ma, Aslam Khan, Lu Wang, Jide Wang, A.S. Maloletnev, Chao Yang, Promotion effects of halloysite nanotubes on catalytic activity of Co_3O_4 nanoparticles toward reduction of 4-nitrophenol and organic dyes, J Hazard Mater., 2021, 403,123870.

[2] Atul Verma, Sanath Kumar, Wen-Ku Chang and Yen-Pei Fu, Bi-functional Ag-Cu_xO/g-C_3N_4 hybrid catalysts for the reduction of 4-nitrophenol and the electrochemical detection of dopamine, Dalton Trans., 2020, 49, 625-637.

[3] Faheem Nawaz, Hongbin Cao, Yongbing Xie, Jiadong Xiao, Yue Chen, Zahid Ali Ghazi, Selection of active phase of MnO_2 for catalytic ozonation of 4-nitrophenol, Chemosphere, 2017, 168, 1457-1466.

[4] Ji-Chao Wang, Ying Li, Heng Li , Zeng-Hui Cui, Yuxia Hou, Weina Shi, Kai Jiang, Lingbo Qu, Yu-Ping Zhang, A novel synthesis of oleophylic Fe_2O_3/polystyrene fibers by γ-Ray irradiation for the enhanced photocatalysis of 4-chlorophenol and 4-nitrophenol degradation, J. Hazard. Mater., 2019, 379, 120806.

[5] Gh. Eshaq, Shaobin Wang, Hongqi Sun, Mika Sillanpaa, Superior performance of $FeVO_4$ @CeO_2 uniform core-shell nanostructures in heterogeneous Fenton-sonophotocatalytic degradation of 4-nitrophenol, J. Hazard. Mater., 2020, 382, 121059.

[6] Mohamed Jaffer Sadiq Mohamed, Sandhya Shenoy U, D. Krishna Bhat, Novel NRGO-CoWO 4-Fe_2O_3 nanocomposite as an efficient catalyst for dye degradation and reduction of 4-nitrophenol, Mater. Chem. Phys., 2018, 208, 112-122.

[7] Mi Yang and Xianyang Shi, Biosynthesis of Ag_2S/TiO_2 nanotubes nanocomposites by Shewanella oneidensis MR-1 for the catalytic degradation of 4-nitrophenol, Environ. Sci. Pollut. Res., 2019, 26, 12237-12246.

[8] hahid Ali Khan, Noureen Khan, Uzma Irum, Aliya Farooq, Abdullah M. Asiri, Esraa M. Bakhsh, Sher Bahadar Khan, Cellulose acetate-Ce/Zr@Cu^0 catalyst for the degradation of organic pollutant, Int. J. Biol. Macromol., 2020, 153, 806-816.

[9] Hongyu Chen, Xiaobin Fan, Jingwen Ma, Guoliang Zhang, Fengbao Zhang and Yang Li, Green Route for Microwave-Assisted Preparation of AuAg-Alloy-Decorated Graphene Hybrids with Superior 4-NP Reduction Catalytic Activity, Ind. Eng. Chem. Res. 2014, 53, 17976-17980.

[10] Guocheng Han, Xiaoyun Li, Jiaming Li, Xiaoying Wang, Yu Shrike Zhang and Runcang Sun, Special Magnetic Catalyst with Lignin-Reduced Au-Pd Nanoalloy, ACS Omega, 2017, 2, 4938-4945.

[11] Jun Xu, Shengli Guo, Lei Jia and Wensheng Zhang, Palygorskite Supported AuPd Alloy Nanoparticles as Efficient Nano-Catalysts for the Reduction of Nitroarenes and Dyes at Room Temperature, Nanomaterials, 2018, 8, 1000.

[12] Sandra Cipagauta-Díaz, Alberto Estrella-González and Ricardo Gómez, Heterojunction formation on $InVO_4$/N-TiO_2 with enhanced visible light photocatalytic activity for reduction of 4-NP, Materials Science in Semiconductor Processing, 2019, 89, 201-211.